LAWRENCE
LIVERMORE
NATIONAL
LABORATORY

LLNL-JRNL-820888

Near-constant retreat rate of a terrestrial margin of the Laurentide Ice Sheet during the last deglaciation

T. V. Lowell, M. A. Kelly, J. A. Howley, T. G. Fisher, P. J. Barnett, R. Schwartz, S. R. H. Zimmerman, N. Norris, A. G. O. Malone

March 25, 2021

Geology

Disclaimer

Near-constant retreat rate of a terrestrial margin of the Laurentide Ice Sheet during the last deglaciation

Thomas V. Lowell[1]*, Meredith A. Kelly[2], Jennifer A. Howley[2], Timothy G. Fisher[3], Peter J. Barnett[4], Roseanne Schwartz[5], Susan R.H. Zimmerman[6], Nathaniel Norris[1] and Andrew G.O. Malone[7]

[1]Department of Geology, University of Cincinnati, Cincinnati, Ohio 45221, USA
[2]Department of Earth Sciences, Dartmouth College, Hanover, New Hampshire 03755, USA
[3]Department of Environmental Sciences, University of Toledo, Toledo, Ohio 43606, USA
[4]Harquail School of Earth Sciences, Laurentian University, Sudbury, Ontario P3E 2C6, Canada
[5]Lamont-Doherty Earth Observatory, Columbia University, Palisades, New York 10964, USA
[6]Center for Accelerator Mass Spectrometry, Lawrence Livermore National Laboratory, Livermore, California 94550, USA
[7]Department of Earth and Environmental Sciences, University of Illinois at Chicago, Illinois 60607, USA

ABSTRACT

The Laurentide Ice Sheet (LIS) was the largest ice sheet during the last glacial period. An accurate representation of its behavior during the last deglaciation is critical to understanding its influence on and response to a changing climate. We use ^{10}Be dating and Bayesian modeling to track the recession of the southwest sector of the Labrador Dome of the LIS along an ~500-km-long transect west of Lake Superior during the last deglaciation. This transect reflects terrestrial ice-margin retreat and crosses multiple moraine sets, with the southwestern part of the transect deglaciated by ca. 19 ka and the northeastern part deglaciated by ca. 10 ka. The predominant behavior of the ice margin during this interval is near-constant retreat with retreat rates varying between ~59 m/a and 38 m/a. The moraine sets mark standstills and/or readvances that in total constitute only ~17% of the retreat interval. The spatial and temporal pattern of ice-margin retreat tracked here differs from existing reconstructions that are based on using isochrons to define ice-margin positions. Acknowledging the uncertainties associated with the modeled ages of ice-margin retreat, we suggest that the overall retreat pattern is consistent with forcing by a gradual increase in Northern Hemisphere, high-latitude summer insolation. The pattern of ice-margin retreat is inconsistent with Greenland ice-core temperature records, and thus these records may not be suitable to drive models of the LIS.

INTRODUCTION

The behavior of ice sheets is interlinked with many key climate processes including atmospheric and oceanic circulation and sea-level changes. The Laurentide Ice Sheet (LIS) was the largest ice sheet during the last glacial period and its topography, albedo, and meltwater influenced climate and other earth systems (e.g., Shapiro et al., 2004; Denton et al., 2010; Ullman et al., 2014; Bacon et al., 2016; Wassenburg et al., 2016). An accurate representation of LIS behavior during a time of dynamic climate change such as the last deglaciation (ca. 20–11 ka) is needed to understand the influence the ice sheet had on the climate system as well as the mechanisms that drove ice-sheet retreat.

The spatial and temporal patterns of LIS retreat are also required input for climate and glaciological models that simulate the deglaciation. Currently, most climate (e.g., Liu et al., 2009; Abe-Ouchi, et al., 2015) and glaciological (e.g., Peltier, 2004; Tarasov et al., 2012) models use a LIS representation that describes ice-margin retreat with isochrons derived from available radiocarbon ages (Dyke, 2004; Dalton et al., 2020). While the available radiocarbon ages were carefully vetted, many of the local study sites were never intended to investigate large-scale patterns of LIS retreat. In addition, for certain time periods and geographic areas, there are few chronologic data that constrain the ice-sheet margin. Therefore, for large sectors of the LIS, the ice-margin retreat patterns and rates are poorly defined.

We present a ^{10}Be chronology of LIS retreat along an ~500-km-long transect perpendicular to the ice-sheet margin during the last deglaciation. We estimate ice-margin retreat rates along this transect using Bayesian modeling of the chronological data. The model results provide spatially continuous retreat rates and quantifiable uncertainties. The transect is approximately parallel to the northeast-southwest ice flow during advance and retreat of the lobe of the southwestern sector of the Labrador Dome (Fig. 1). Its location, from northeastern Minnesota, USA, to northwestern Ontario, Canada, tracks terrestrial ice-margin recession away from former ice streams and across an upland surface at a higher elevation than any former glacial lakes (e.g., Glacial Lake Agassiz) and Lake Superior to avoid a calving influence on ice-margin retreat.

METHODS

We determined the timing of deglaciation along the transect by dating glacially transported boulders with the cosmogenic nuclide ^{10}Be (hereinafter referred to as ^{10}Be dating; Fig. 1; see the Supplemental Material[1]). ^{10}Be ages are calculated using the online calculator formerly known as the CRONUS-Earth online calculator v3 (Balco et al., 2008) with the Northeast North America production rate (Balco et al., 2009) and

*E-mail: Thomas.lowell@uc.edu

[1]CITATION: Lowell, T.V., et al., 2021, Near-constant retreat rate of a terrestrial margin of the Laurentide Ice Sheet during the last deglaciation: Geology, v. 49, p., https://doi.org/10.1130/G49081.1

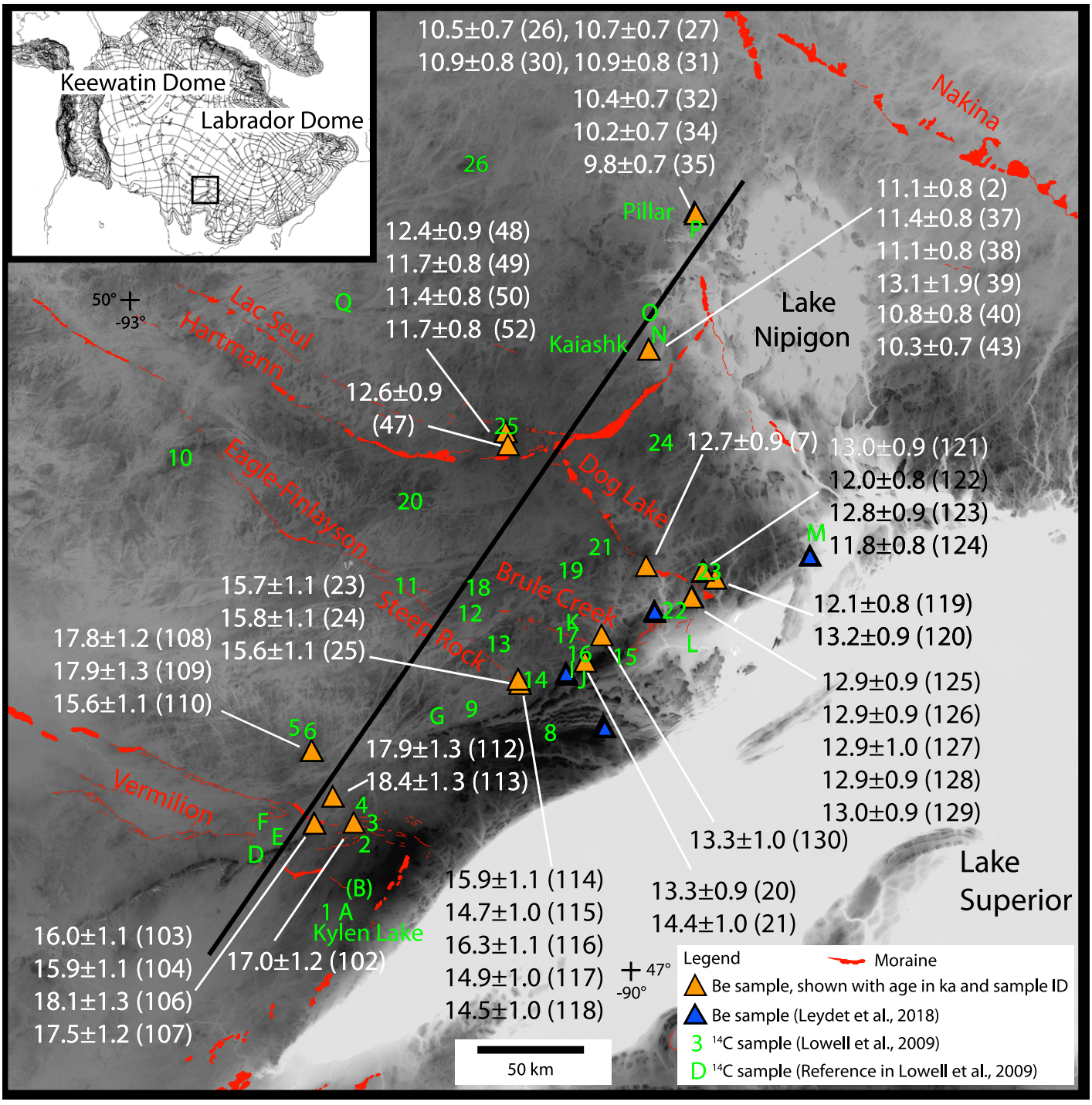

Figure 1. Map showing the locations of moraines (red areas), chronological data, and the transect (black line) along which we determined Laurentide Ice Sheet deglaciation. Moraine names are in red. Also shown (in green) are the locations of the Kelly et al. (2016) study sites in the Kaiashk and Pillar channel complexes and Kylen Lake (Norris, 2019). ^{10}Be ages are shown with external uncertainties, and adjacent numbers in brackets refer to sample numbers in Tables S1–S3 (see footnote 1). Green letters and numbers are sites of radiocarbon samples coded to table 1 of Lowell et al. (2009), and blue triangles are sites of ^{10}Be samples from Leydet et al. (2018).

the time-independent ("St") scaling scheme of Lal (1991) and Stone (2000) (Table S3). The choice of scaling scheme does not significantly change the ^{10}Be ages. The ^{10}Be ages are calculated assuming an erosion rate of 0.0003 cm/a and are not corrected for post-glacial isostatic uplift (Tables S3 and S4). We extend the transect to the southwest by including a basal radiocarbon age from Kylen Lake, Minnesota (Birks, 1981; Lund and Banerjee, 1985; Norris, 2019; see the Supplemental Material). At the northeastern end of the transect, we include recalculated ^{10}Be ages of boulders in the Kaiashk and Pillar channel complexes, which are located west and northwest of Lake Nipigon, respectively, from Kelly et al. (2016) (Table S3).

The transect crosses major moraine sets consisting of multiple and, in places, cross-cutting ridges (i.e., the Vermilion Moraine; Steep Rock, Eagle-Finlayson, and Brule Creek Moraines; Dog Lake Moraine; and Lac Seul Moraine; Zoltai, 1965; Fig. 1) that record either ice-margin stillstands or readvances. By dating boulders on and between the sets of moraines, we examine ice-margin retreat rates over the entire transect and estimate the duration of stillstands and/or readvances. Using the geomorphic relationships

of the moraines—specifically that moraines are progressively younger to the northeast—we assume that the ^{10}Be chronology of deglaciation is analogous to vertical accretion of radiocarbon-dated sediment within a lake. Based on this assumption, we employ a Bayesian modeling approach (Blaauw and Christen, 2011) using all (51) ^{10}Be ages to determine retreat rates and assign ages to the moraines (see the Supplemental Material). We modeled ice-margin recession without and with hiatuses at the moraine locations, but since a moraine records an ice-margin stillstand or readvance, we prefer the model with hiatuses.

RESULTS

The ^{10}Be ages with external uncertainties (i.e., measurement and ^{10}Be production-rate uncertainties) are shown along the transect (Fig. 1) and reported below. The model results yield age estimates for deglaciation that we use throughout the discussion (Fig. 2). Modeling with hiatuses shows that the external uncertainties of ^{10}Be ages translate to mean errors of +0.7 ka and −0.6 ka (at the 95% confidence level) in the modeled ages. The magnitude of the modeled age errors varies along the transect, with errors along the southern, older portion of the transect larger than along the northern, younger portion of the transect.

The southwestern end of the transect is anchored by the Kylen Lake site, where Bayesian modeling of radiocarbon ages with depth indicates deglaciation by 18.1 + 0.6/–0.4 cal kyr B.P. (Fig. 1; see the Supplemental Material). Northeastward from this site, 51 ^{10}Be ages show a distinct pattern of retreat from the Vermilion Moraine to the north end of Lake Nipigon. ^{10}Be ages of boulders on and north of the Vermilion Moraine range from 18.4 ± 1.3–15.6 ± 1.1 ka (n = 10). ^{10}Be ages near the Steep Rock, Eagle-Finlayson, and Brule Creek Moraines indicate deglaciation between 16.3 ± 1.1 ka and 13.3 ± 0.9 ka (n = 11). ^{10}Be ages of boulders just south of the Dog Lake Moraine are 13.0 ± 0.9–12.9 ± 0.9 ka (n = 5), and those just north of the moraine are 13.2 ± 0.9–11.8 ± 0.8 (n = 6). ^{10}Be ages between the Hartmann and Lac Seul Moraines indicate deglaciation between 12.6 ± 0.9 ka and 11.4 ± 0.8 ka (n = 5). The Kaiashk and Pillar channel complexes were exposed at 11.3 ± 1.0 ka (n = 6) and 10.5 ± 0.4 ka (n = 7), respectively (Kelly et al., 2016).

The model assuming no hiatuses yields a constant mean retreat rate of ~46 m/a (Supplemental Material). The preferred model (with hiatuses) shows ice-margin retreat from the Vermilion Moraine at 17.5 ± 0.6 ka, the Eagle-Finlayson Moraine at 14.7 ± 0.7 ka, the Dog Lake Moraine at 12.7 ± 0.4 ka, and the Lac Seul Moraine at 12.1 ± 0.4 ka. The model-estimated retreat rate between Kylen Lake and the Vermilion Moraine is ~59 m/a, between the Vermilion and Steep Rock Moraines is ~52 m/a, between the Eagle-Finlayson and Dog Lake Moraines is ~38 m/a, between the Dog Lake and Lac Seul Moraines is ~55 m/a, and north of the Lac Seul Moraine is ~55 m/a. Moraine hiatus durations are ~499 a for the Vermilion Moraine; ~607 a for the Steep Rock, Eagle-Finlayson, and Brule Creek Moraines; ~228 a for the Dog Lake Moraine; and ~93 a for the Lac Seul Moraine.

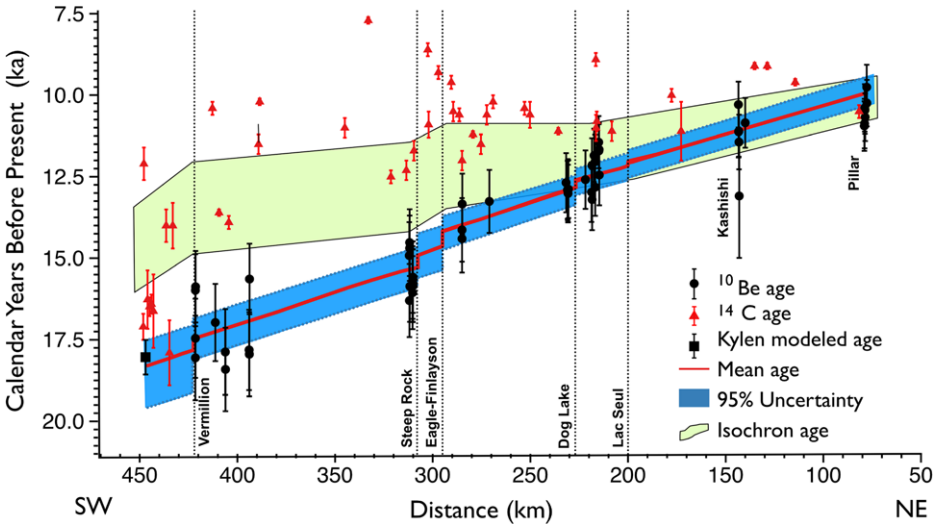

Figure 2. Time-distance graph showing the chronological constraints on Laurentide Ice Sheet deglaciation along the transect (see Fig. 1 for transect location). The x-axis is distance along the transect set up to mimic the stratigraphic order in sediment cores necessary for the Bacon analysis. Moraine locations (dotted vertical lines) are indicated. Black circles and lines are ^{10}Be ages and external uncertainties (Fig. 1; see the Supplemental Material [see footnote 1]). Red triangles and lines are radiocarbon ages reported in table 1 of Lowell et al. (2009; see Fig. 1 for sample locations). Red line is the weighted mean of all possible retreat patterns, and the uncertainty envelope is shown in blue. The steps in the red line represent the durations of hiatuses. Isochrons and associated uncertainty envelope (light green shading) are from Dalton et al. (2020) with radiocarbon ages converted to calendar years.

DISCUSSION

The modeling results indicate that the dominant behavior of the southwestern sector of the Labrador Dome was near-constant retreat between ca. 19 ka and 10 ka with an average retreat rate of ~52 m/a for ~83% of the time. The moraines represent a total hiatus duration of ~1.4 ka (~17% of the time) and are interpreted as minor interruptions in the overall pattern of retreat. The Vermilion Moraine is composed of at least four moraine ridges (Lehr and Hobbs, 1992) and may represent brief standstills of the ice-sheet margin. The Steep Rock, Eagle-Finlayson, and Brule Creek Moraines show the longest duration hiatus (~607 a) between 15.3 ± 0.6 ka and 14.7 ± 0.7 ka. Mapping by Zoltai (1965) shows the Brule Creek Moraine truncating an unnamed moraine between it and the Steep Rock Moraine and parts of the Eagle-Finlayson Moraine overlapping the Steep Rock Moraine. Therefore, at least some moraines in this set register readvances. Ice-flow indicators proximal to the Dog Lake Moraine indicate that it represents a readvance (Zoltai, 1965) that we estimate to have occurred between 12.9 ± 0.5 ka and 12.7 ± 0.4 ka. The Lac Seul Moraine makes up the shortest duration hiatus (~93 a) and likely represents a brief standstill or minor readvance. Similar to our finding of near-constant retreat rates, Breckenridge et al. (2021) determined a near-constant LIS retreat rate during the Pleistocene-Holocene transition using glacial varves in the Glacial Lake Agassiz basin. However, the retreat rate in Breckenridge et al. (2021), which was determined in an area where the moraines are more closely spaced, is slower (25 m/a) and occurs over a shorter time interval (~1.5 ka).

The pattern of ice retreat reconstructed here is different from those using the radiocarbon-based isochron method, including the commonly used LIS deglaciation model of Dyke (2004) and revised model of Dalton et al. (2020) (Fig. 2). For example, the isochrons of Dalton et al. (2020) range from ca. 4 ka younger than our deglaciation ages near the Vermilion Moraine to ca. 1.4 ka younger at the Dog Lake and Lac Seul Moraines. One interpretation of this offset is that organic sedimentation on the landscape occurred at ca. 4–1.4 ka after deglaciation. However, there is reasonable agreement between the radiocarbon and ^{10}Be ages of deglaciation south of the Vermilion Moraine and north of the Dog Lake and Lac Seul Moraines. We suggest that organic material on the landscape was less common subsequent to deglaciation in some areas along the transect and, therefore, is less likely to be recovered by lake coring.

Based on the spatial and temporal discord between our ice-margin reconstruction and the isochrons, we urge caution when using the isochron data in LIS reconstructions in glaciological and climate models. For example, the TraCE-21ka transient climate simulation (https://www.cgd.ucar.edu/ccr/TraCE/) provides the basis for important paleoclimate interpretations about the causes of deglacial warming and abrupt climate events (Liu et al., 2009, 2012). However, the TraCE-21ka simulation uses ice-boundary conditions of ICE-5G (VM2) (Peltier, 2004), which generated ice thicknesses over time using the isochrons of Dyke (2004). Within the model grid cell that includes the transect studied here, there was an ice sheet ~2000 m high over much of the area until ca. 14 ka (Fig. 3). We suggest that the ice-boundary input data for this and other climate simulations needs to be improved to reconstruct past climate conditions more accurately and, thus, better understand the mechanisms of climate change.

We evaluated possible drivers of ice-margin retreat documented but recognize that the age-model uncertainties (ca. ± 0.7 ka) hinder any correlations with abrupt climate changes. The overall retreat pattern is compatible with Northern Hemisphere, high-latitude summer insolation and atmospheric greenhouse gas concentrations as major forcings (Fig. 3). Since ice-margin retreat is driven by ablation, we used a simple energy balance algorithm that includes both insolation and summer duration to compute the total positive degree days (PDD) per year (Huybers and Tziperman, 2008). For the study area, these estimates have a nearly linear increase in PDD per year from ca. 18–13.5 ka, and a slight decrease after 11 ka. Atmospheric greenhouse gas concentrations show a similar increase beginning at ca. 18 ka with a pause in the increase at ca. 14.5–12.9 ka (Marcott et al., 2014).

Many studies use Greenland ice core oxygen-isotope records as a proxy for regional or even hemispheric climate conditions during the last deglaciation (e.g., Marshall et al., 2002; Tarasov and Peltier, 2004; Gregoire et al., 2012). However, a comparison of the North Greenland Ice Core Project (NGRIP) temperature record (Buizert et al., 2014) with LIS deglaciation tracked here shows little to no correspondence (Fig. 3). The near-constant retreat rate does not resemble the step-like changes of nearly glacial/interglacial magnitude observed in Greenland ice-core temperatures during the warm Bølling-Allerød period (14.5–12.9 ka) and cold Younger Dryas event (12.9–11.7 ka). In contrast, the ice-margin retreat rate during the Bølling-Allerød (~38 m/a) is slower than those occurring at ca. 17–15 ka (~52 m/a) and during the Younger Dryas event (~55 m/a).

CONCLUSIONS

The behavior of the southwestern sector of the Labrador Dome from ca. 19–10 ka was predominantly retreat, with nearly constant retreat rates between short times of moraine deposition. Multiple moraine sets represent sub-millennial-scale ice-sheet standstills and/or readvances that make up only ~17% of the total duration of deglaciation. The pattern and timing of ice-margin retreat documented here differ from those determined using the isochron method. We caution against using LIS reconstructions based on the isochron method as input for climate models and targets for glaciological modeling. The pattern of retreat resembles the gradual increase in Northern Hemisphere, high-latitude summer insolation and, to some extent, the rise in atmospheric greenhouse gas concentrations during the last deglaciation. It does not correspond with the pattern of temperature changes registered by Greenland ice cores.

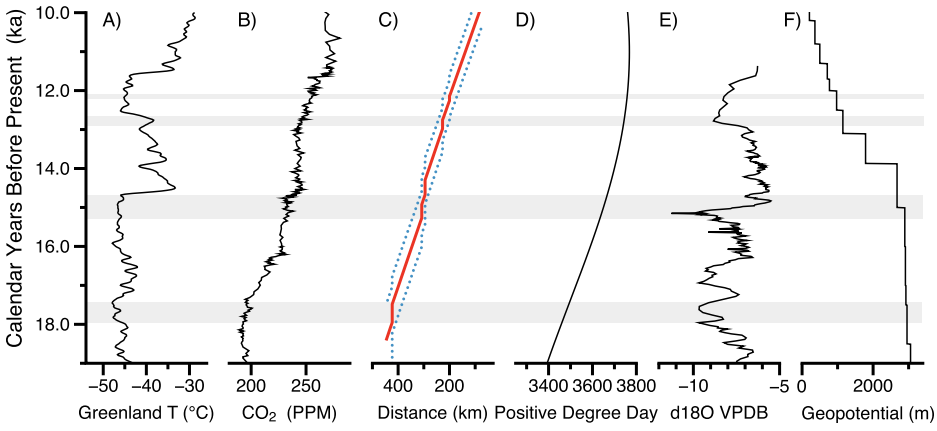

Figure 3. Comparison of the simplified time-distance graph with climate proxy records. (A) Greenland temperatures derived from $\delta^{15}N$ values using the North Greenland Ice Core Project ss09sea06bm time scale (Kindler et al., 2014). (B) Atmospheric CO_2 from the West Antarctic Ice Sheet Divide ice core (Marcott et al., 2014). (C) Simplication of the deglaciation model in Figure 2. (D) Total summer positive degree days (PDD; Huybers and Tziperman, 2008). (E) Precipitation changes from a speleothem near Fort Stanton, New Mexico, USA, that is inferred to represent changes in the polar jet stream (Asmerom et al., 2010). (F) Surface geopotential height extracted as a surrogate for surface elevation from the TraCE-21ka simulation (Liu et al., 2009) for the grid cell nearest to the study site (center latitude: 50.1°N, center longitude: 90°W). The TraCE-21ka surface-elevation changes reflect the thickness of the Laurentide Ice Sheet in the model as prescribed by the ICE-5G (VM2) reconstruction (Peltier, 2004). The gray horizontal bars represent the hiatuses modeled. PPM—parts per million; VPDB—Vienna Pee Dee belemnite.

ACKNOWLEDGMENTS

We are grateful for generous support from the Comer Family Foundation (Chicago, Illinois, USA) including grants to T. Lowell (CP28, CP39), M. Kelly (CP73), and T. Fisher (CP29). ^{10}Be samples were processed at Lamont-Doherty Earth Observatory (Palisades, New York) and Dartmouth College (Hanover, New Hampshire). We thank E. Putnam and C. Quinn for laboratory assistance at Dartmouth College. We thank the editor, C. Clark, as well as B. Laabs and two anonymous reviewers for thoughtful critiques. This is LLNL-JRNL-820888.

REFERENCES CITED

Abe-Ouchi, A., et al., 2015, Ice-sheet configuration in the CMIP5/PMIP3 Last Glacial Maximum experiments: Geoscientific Model Development, v. 8, p. 3621–3637, https://doi.org/10.5194/gmd-8-3621-2015.

Asmerom, Y., Polyak, V.J., and Burns, S.J., 2010, Variable winter moisture in the southwestern United States linked to rapid glacial climate shifts: Nature Geoscience, v. 3, p. 114–117, https://doi.org/10.1038/ngeo754.

Bacon, C.D., Molnar, P., Antonelli, A., Crawford, A.J., Montes, C., and Vallejo-Pareja, M.C., 2016, Quaternary glaciation and the Great American Biotic Interchange: Geology, v. 44, p. 375–378, https://doi.org/10.1130/G37624.1.

Balco, G., Stone, J.O., Lifton, N.A., and Dunai, T.J., 2008, A complete and easily accessible means of calculating surface exposure ages or erosion rates from ^{10}Be and ^{26}Al measurements: Quaternary Geochronology, v. 3, p. 174–195, https://doi.org/10.1016/j.quageo.2007.12.001.

Balco, G., Briner, J., Finkel, R.C., Rayburn, J.A., Ridge, J.C., and Schaefer, J.M., 2009, Regional beryllium-10 production rate calibration for late-glacial northeastern North America: Quaternary Geochronology, v. 4, p. 93–107, https://doi.org/10.1016/j.quageo.2008.09.001.

Birks, H.J.B., 1981, Late Wisconsin vegetational and climatic history at Kylen Lake, northeastern Minnesota: Quaternary Research, v. 16, p. 322–355, https://doi.org/10.1016/0033-5894(81)90015-6.

Blaauw, M., and Christen, J.A., 2011, Flexible paleoclimate age-depth models using an autoregressive gamma process: Bayesian Analysis, v. 6, p. 457–474, https://doi.org/10.1214/ba/1339616472.

Borchers, B., Marrero, S., Balco, G., Caffee, M., Goehring, B., Lifton, N., Nishiizumi, K., Phillips, F., Schaefer, J., and Stone, J., 2016, Geological calibration of spallation production rates in the CRONUS-Earth project: Quaternary Geochronology, v. 31, p. 188–198, https://doi.org/10.1016/j.quageo.2015.01.009.

Breckenridge, A., Lowell, T.V., Wattrus, N., Moretto, M., Norris, N., and Dennison, A., 2021, A new glacial varve chronology along the southern

Laurentide Ice Sheet that spans the Younger Dryas–Holocene boundary: Geology, v. 49, p. 283–288, https://doi.org/10.1130/G47995.1.

Buizert, C., et al., 2014, Greenland temperature response to climate forcing during the last deglaciation: Science, v. 345, p. 1177–1180, https://doi.org/10.1126/science.1254961.

Dalton, A.S., et al., 2020, An updated radiocarbon-based ice margin chronology for the last deglaciation of the North American Ice Sheet Complex: Quaternary Science Reviews, v. 234, 106223, https://doi.org/10.1016/j.quascirev.2020.106223.

Denton, G.H., Anderson, R.F., Togweiler, J.R., Edwards, R.L., Schaefer, J.M., and Putnam, A.E., 2010, The last glacial termination: Science, v. 328, p. 1652–1656, https://doi.org/10.1126/science.1184119.

Dyke, A.S., 2004, An outline of North American deglaciation with emphasis on central and northern Canada, *in* Ehlers, J., and Gibbard, P.L., eds., Quaternary Glaciations—Extent and Chronology, Part II North America: Amsterdam, Elsevier B.V., p. 373, https://doi.org/10.1016/S1571-0866(04)80209-4.

Gregoire, L.J., Payne, A.J., and Valdes, P.J., 2012, Deglacial rapid sea level rises caused by ice-sheet saddle collapses: Nature, v. 487, p. 219–222, https://doi.org/10.1038/nature11257.

Huybers, P., and Tziperman, E., 2008, Integrated summer insolation forcing and 40,000-year glacial cycles: The perspective from an ice-sheet/energy-balance model: Paleoceanography, v. 23, PA1208, https://doi.org/10.1029/2007PA001463.

Kelly, M.A., Fisher, T.G., Lowell, T.V., Barnett, P.J., Schwartz, R., and Gajewski, K., 2016, ^{10}Be ages of flood deposits west of Lake Nipigon, Ontario: Evidence for eastward meltwater drainage during the early Holocene Epoch: Canadian Journal of Earth Sciences, v. 53, p. 321–330, https://doi.org/10.1139/cjes-2015-0135.

Kindler, P., Guillevic, M., Baumgartner, M., Schwander, J., Landais, A., Leuenberger, M., Spahni, R., Capron, E., and Chappellaz, J., 2014, Temperature reconstruction from 10 to 120 kyr b2k from the NGRIP ice core: Climate of the Past, v. 10, p. 887–902, https://doi.org/10.5194/cp-10-887-2014.

Lal, D., 1991, Cosmic ray labeling of erosion surfaces: In situ nuclide production rates and erosion models: Earth and Planetary Science Letters, v. 104, p. 424–439, https://doi.org/10.1016/0012-821X(91)90220-C.

Leydet, D.J., Carlson, A.E., Teller, J.T., Breckenridge, A., Barth, A.M., Ullman, D.J., Sinclair, G., Milne, G.A., Cuzzone, J.K., and Caffee, M.W., 2018, Opening of glacial Lake Agassiz's eastern outlets by the start of the Younger Dryas cold period: Geology, v. 46, p. 155–158, https://doi.org/10.1130/G39501.1.

Lehr, J.D., and Hobbs, H.C., 1992, Guidebook 18. Field Trip Guidebook Glacial Geology of the Laurentian Divide Area, St. Louis and Lake Counties, Minnesota: Minneapolis, Minnesota Geological Survey, 73 p.

Liu, Z., et al., 2009, Transient simulation of last deglaciation with a new mechanism for Bolling-Allerod warming: Science, v. 325, p. 310–314, https://doi.org/10.1126/science.1171041.

Liu, Z., et al., 2012, Younger Dryas cooling and the Greenland climate response to CO_2: Proceedings of the National Academy of Sciences of the United States of America, v. 109, p. 11,101–11,104, https://doi.org/10.1073/pnas.1202183109.

Lowell, T.V., Fisher, T.G., Hajdas, I., Glover, K., Loope, H., and Henry, T., 2009, Radiocarbon deglaciation chronology of the Thunder Bay, Ontario area and implications for ice sheet retreat patterns: Quaternary Science Reviews, v. 28, p. 1597–1607, https://doi.org/10.1016/j.quascirev.2009.02.025.

Lund, S.P., and Banerjee, S.K., 1985, Late Quaternary paleomagnetic field secular variation from two Minnesota Lakes: Journal of Geophysical Research: Solid Earth, v. 90, B1, p. 803–825, https://doi.org/10.1029/JB090iB01p00803.

Marcott, S.A., et al., 2014, Centennial-scale changes in the global carbon cycle during the last deglaciation: Nature, v. 514, p. 616–619, https://doi.org/10.1038/nature13799.

Marshall, S.J., James, T.S., and Clarke, G.K.C., 2002, North American Ice Sheet reconstructions at the Last Glacial Maximum: Quaternary Science Reviews, v. 21, p. 175–192, https://doi.org/10.1016/S0277-3791(01)00089-0.

Norris, N., 2019, The Mystery Interval: Hydrologic changes and circulation pattern changes? [M.S. thesis]: Cincinatti, Ohio, University of Cincinnati, 63 p.

Peltier, W.R., 2004, Global glacial isostasy and the surface of the Ice-Age Earth: The ICE-5G (VM2) model and GRACE: Annual Review of Earth and Planetary Sciences, v. 32, p. 111–149, https://doi.org/10.1146/annurev.earth.32.082503.144359.

Shapiro, B., et al., 2004, Rise and fall of the Beringian Steppe bison: Science, v. 306, p. 1561–1565, https://doi.org/10.1126/science.1101074.

Stone, J.O., 2000, Air pressure and cosmogenic isotope production: Journal of Geophysical Research: Solid Earth, v. 105, B10, p. 23,753–23,759, https://doi.org/10.1029/2000JB900181.

Tarasov, L., and Peltier, W.R., 2004, A geophysically constrained large ensemble analysis of the deglacial history of the North American ice-sheet complex: Quaternary Science Reviews, v. 23, p. 359–388, https://doi.org/10.1016/j.quascirev.2003.08.004.

Tarasov, L., Dyke, A.S., Neal, R.M., and Peltier, W.R., 2012, A data-calibrated distribution of deglacial chronologies for the North American ice complex from glaciological modeling: Earth and Planetary Science Letters, v. 315–316, p. 30–40, https://doi.org/10.1016/j.epsl.2011.09.010.

Ullman, D.J., LeGrande, A.N., Carlson, A.E., Anslow, F.S., and Licciardi, J.M., 2014, Assessing the impact of Laurentide Ice Sheet topography on glacial climate: Climate of the Past, v. 10, p. 487–507, https://doi.org/10.5194/cp-10-487-2014.

Wassenburg, J.A., et al., 2016, Reorganization of the North Atlantic Oscillation during early Holocene deglaciation: Nature Geoscience, v. 9, p. 602–605, https://doi.org/10.1038/ngeo2767.

Zoltai, S.C., 1965, Glacial features of the Quetico-Nipigon area, Ontario: Canadian Journal of Earth Sciences, v. 2, p. 247–269, https://doi.org/10.1139/e65-021.